Heterogeneous Catalysis

DOI: 10.1002/anie.201402342

Maximum Noble-Metal Efficiency in Catalytic Materials: Atomically Dispersed Surface Platinum**

Albert Bruix, Yaroslava Lykhach, Iva Matolínová, Armin Neitzel, Tomáš Skála, Nataliya Tsud, Mykhailo Vorokhta, Vitalii Stetsovych, Klára Ševčíková, Josef Mysliveček, Roman Fiala, Michal Václavů, Kevin C. Prince, Stéphanie Bruyère, Valérie Potin, Francesc Illas, Vladimír Matolín, Jörg Libuda,* and Konstantin M. Neyman**

Abstract: *Platinum is the most versatile element in catalysis, but it is rare and its high price limits large-scale applications, for example in fuel-cell technology. Still, conventional catalysts use only a small fraction of the Pt content, that is, those atoms located at the catalyst's surface. To maximize the noble-metal efficiency, the precious metal should be atomically dispersed and exclusively located within the outermost surface layer of the material. Such atomically dispersed Pt surface species can indeed be prepared with exceptionally high stability. Using DFT calculations we identify a specific structural element, a ceria "nanopocket", which binds Pt^{2+} so strongly that it withstands sintering and bulk diffusion. On model catalysts we experimentally confirm the theoretically predicted stability, and on real Pt-CeO_2 nanocomposites showing high Pt efficiency in fuel-cell catalysis we also identify these anchoring sites.*

Platinum is one of the most versatile elements in catalysis, efficiently mediating a multitude of chemical reactions.[1] The fabrication of three-way catalysts for gasoline-powered vehicles alone consumes more than one third of the globally produced Pt and constitutes an annual worldwide market of several billion US$.[2] Furthermore, Pt is very rare (0.003 ppb in the earth crust) and its market price (around 1500 US$/oz) generally exceeds that of gold. Such excessive costs are the foremost problem when commercializing new industrial applications featuring Pt-containing materials as catalysts.[3] For instance, the high price and demand for Pt is one of the major obstacles limiting large-scale application of fuel-cell technology.[3,4]

Not surprisingly, the goal of reducing the demand for Pt (and other platinum-group metals, PGM) is a major driving force in catalysis research.[5] There are two strategies to tackle this challenge: The first is the replacement of precious noble metals by new, less-expensive, and more-abundant materials. Promising strategies have been proposed[6] but so far many noble-metal-free catalysts cannot compete with their expensive counterparts. The second strategy—straightforward and simple—has been followed ever since noble metals have been used in heterogeneous catalysis: The idea is to use the expensive metal as efficiently as possible.[7] In this case, the most critical parameter is the dispersion, that is, the fraction of the metal atoms that are exposed to reactants.[8] Small PGM nanoparticles (NPs) supported on high-surface-area

[*] Dr. A. Bruix, Prof. Dr. F. Illas, Prof. Dr. K. M. Neyman
Departament de Química Física and Institut de Química Teòrica i Computacional (IQTCUB), Universitat de Barcelona
c/Martí i Franquès 1, 08028 Barcelona (Spain)
Prof. Dr. K. M. Neyman
Institució Catalana de Recerca i Estudis Avançats (ICREA)
Pg. Lluís Companys 23, 08010 Barcelona (Spain)
E-mail: konstantin.neyman@icrea.cat
Dr. Y. Lykhach, M. Sc. A. Neitzel, Prof. Dr. J. Libuda
Lehrstuhl für Physikalische Chemie II
Friedrich-Alexander-Universität Erlangen-Nürnberg (Germany)
Prof. Dr. J. Libuda
Erlangen Catalysis Resource Center
Friedrich-Alexander-Universität Erlangen-Nürnberg
Egerlandstrasse 3, 91058 Erlangen (Germany)
E-mail: joerg.libuda@fau.de
Dr. I. Matolínová, Dr. T. Skála, Dr. N. Tsud, Dr. M. Vorokhta, M. Sc. V. Stetsovych, M. Sc. K. Ševčíková, Dr. J. Mysliveček, M. Sc. R. Fiala, M. Sc. M. Václavů, Prof. Dr. V. Matolín
Department of Surface and Plasma Science, Charles University
V Holešovičkách 2, 18000 Prague (Czech Republic)
E-mail: matolin@mbox.troja.mff.cuni.cz
Dr. S. Bruyère, Dr. V. Potin
Laboratoire Interdisciplinaire Carnot de Bourgogne, UMR 6303 CNRS-Université de Bourgogne
9 Av. A. Savary, BP 47870, 21078 Dijon Cedex (France)
Dr. K. C. Prince
Sincrotrone Trieste SCpA and IOM
Strada Statale 14, km 163.5, 34149 Basovizza-Trieste (Italy)

[**] We acknowledge financial support by the EU (FP7 NMP project ChipCAT No. 310191 and COST Action CM1104), the Spanish MINECO (grants CTQ2012-34969, CTQ2012-30751, FIS2008-02238) and MICINN (grant BES-2009-021571 for A.B.), French ANR within the IMAGINOXE project (ANR-11-JS10-001) as well as the Czech Science Foundation grants P204/11/1183 and 13-10396S. K.M.N. thanks Alexander von Humboldt Foundation for financing his research stay in Erlangen and F.I. acknowledges additional financial support through the 2009 ICREA Academia Award for Excellence in University Research. Additional financial support by the Deutsche Forschungsgemeinschaft (DFG) within the Excellence Cluster "Engineering of Advanced Materials" in the framework of the excellence initiative is acknowledged. Computer resources were partly provided by the Red Española de Supercomputación. The Materials Science Beamline is supported by the LG12003 project of the Czech Ministry of Education.

Supporting information for this article is available on the WWW under http://dx.doi.org/10.1002/anie.201402342.

oxides are commonly employed in catalytic materials to achieve high dispersion. Yet, it is still only a minor fraction of the metal that is truly active in most reactions.

How should we design an "ideal catalytic material" that makes the maximum use of the noble-metal component? In this ideal material each individual precious-metal atom should be accessible to reactants. In other words, the entire noble-metal content should be dispersed in the form of atoms located in the very surface layer of the catalyst material.[9] In fact, it was recently discovered that traces of atomically dispersed platinum (and gold) on ceria are catalytically active.[10] This and similar systems represent a new class of catalysts—atomically dispersed supported metal catalysts.[11]

Yet it is not enough to just prepare an atomically dispersed catalyst. Under the harsh conditions of many catalytic reactions, two phenomena often lead to rapid deactivation: sintering of the particles and bulk diffusion of the active metal reduce the fraction of surface atoms. Consequently, the "ideal catalytic material" must also stabilize the active metal atoms against agglomeration and bulk diffusion. In other words, we need to anchor the atomically dispersed active atoms at the surface so strongly that they will resist both the aggregation into NPs and the diffusion into deeper layers.

Herein, combining theory and experiment, we have identified a target structure for an atomically dispersed Pt catalyst that fulfills both requirements. By means of density-functional theory (DFT) calculations we determine a structural element with unique properties: a surface Pt^{2+} ion that resides in a square-planar coordination site located at a CeO_2 nanofacet. Theory predicts that this structural unit should be so stable that it will resist aggregation into metallic Pt NPs. Moreover, it can only be formed at the surface, thus preventing Pt diffusion into the bulk. By model catalytic experiments in ultrahigh vacuum (UHV) we show that these Pt^{2+} centers do exist at the surface and indeed feature the predicted stability. On real ceria NPs prepared by thin film technologies, we identify the same Pt^{2+} species and locate the {100} nanofacets where these atomically dispersed species are stabilized.

In Figure 1 we summarize the results from the DFT studies. We start our quest for the "ideal" Pt site by analyzing suitable ceria NPs. Recently, we have shown that the ceria nanostructure critically controls its surface properties.[12] We have identified the cuboctahedral $Ce_{40}O_{80}$ NP as a representative model for nanostructured ceria (Figure 1).[13] It features a truncated octahedral shape with O-terminated {111} and very small {100} nanofacets. The {100} nanofacets correspond to the polar (100) surface, which is notably less stable than the (111) surface of ceria.[14] Yet, these {100} nanofacets are abundant structural elements on nanostructured ceria.[13a,b] As we will show, they turn out to play the key role in this study.

Atomic Pt is placed on various sites of the $Ce_{40}O_{80}$ NP. We find a moderately strong binding (adsorption energy of −273 to −303 kJ mol^{-1}) on the {111} facets, resulting in Pt^0 and Pt^+ states, respectively (see supplementary online text for more

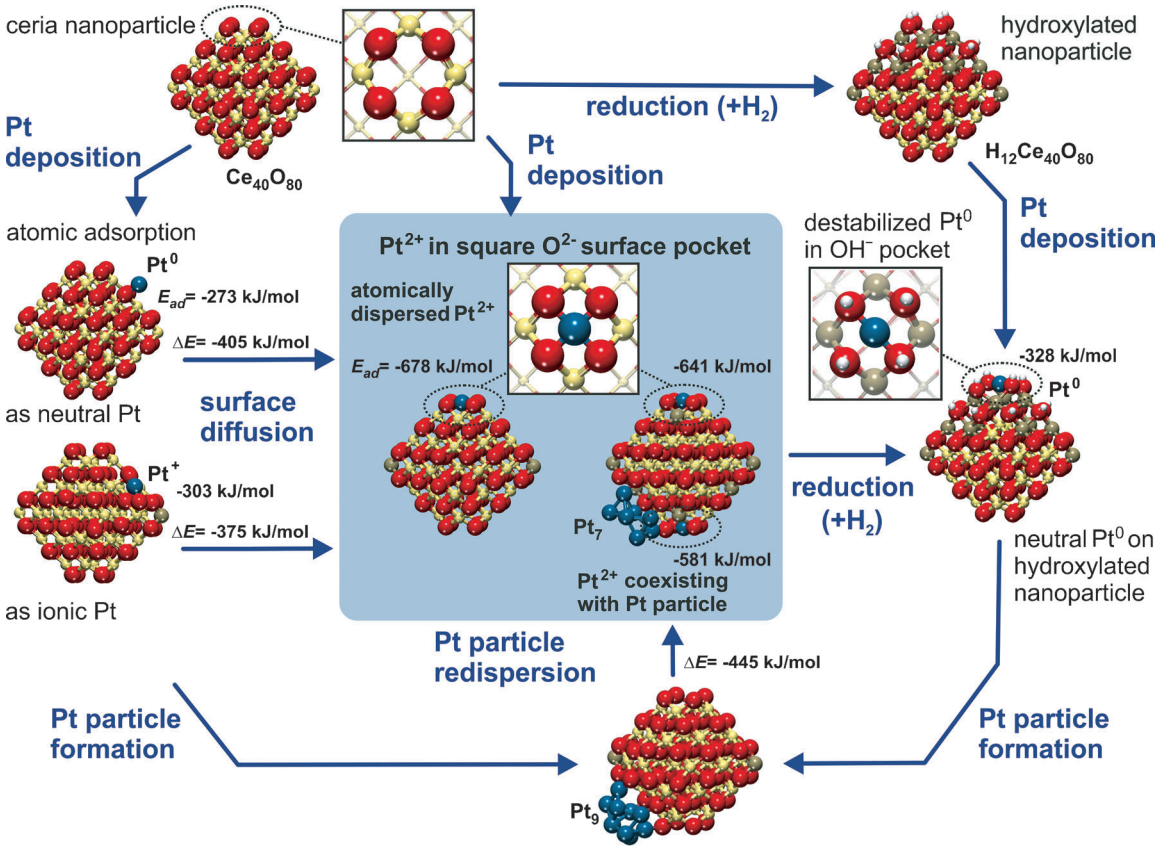

Figure 1. Structure and energetics of the anchored Pt^{2+} species on ceria nanoparticles determined by theory. The Pt^{2+} is strongly bound at the {100} nanofacets of the ceria nanoparticle. Color coding of atoms: red O, beige Ce^{4+}, brown Ce^{3+}, blue Pt, white H.

details). The adsorption energy is similar to that calculated on the regular $CeO_2(111)$ surface ($-256\ kJ\,mol^{-1}$).[15] The formal charge state of Pt is determined by the number of Ce cations reduced upon the adsorption, that is, $Ce^{4+}(4f^0) \rightarrow Ce^{3+}(4f^1)$.

Surprisingly, the atomic Pt adsorbed on the {100} nanofacet turns out to behave entirely differently. It acquires a 2+ state by donation of two electrons, thereby creating two Ce^{3+} centers (Figure 1). Most importantly, the adsorption energy is extraordinarily large: the Pt^{2+} is bound to the oxide by as much as $678\ kJ\,mol^{-1}$. Such strong interactions of metal atoms with oxide surfaces are indicative of surface coordination compounds, in which the support acts as a polydentate ligand.[16] Apparently, the "surface pocket" with the four O^{2-} ions (nearest neighbor separations of 315–320 pm, see Figure S1a in the Supporting Information) provides an ideal "matrix" to host the $Pt^{2+}(d^8)$ ion.[17] Indeed, our calculations reveal the formation of a nearly square-planar arrangement with the central atom Pt^{2+} elevated by just 11 pm over the plane of the surface O anions. Upon binding to the Pt atom, the O^{2-} square contracts to the nearest neighbor separations of 289–290 pm, leading to Pt–O distances of 205 pm (Figure S1b). Such contraction requires substantial structural flexibility which is, however, easily provided by the nanoparticle. Note that the O-terminated {100} facets are not the only sites on the NP that could accommodate Pt^{2+} ions in a square-planar coordination. The same local PtO_4 structure (featuring Pt^{2+}, Figure S1d) results from the substitution of a corner Ce atom of the NP by Pt atom accompanied by the release of an O atom. We note that in previous EXAFS (extended X-ray absorption fine structure) studies on real catalysts it was speculated that atomic Pt may indeed be located in a square-planar arrangement of oxygen ions.[18] Our DFT calculations identify the atomic structure of these sites and reveal their striking stability.

Remarkable consequences arise from the strong anchoring of the Pt^{2+} ions at the {100} "nanopockets". These are summarized in Figure 1. The adsorption energy of the anchored Pt^{2+} ion exceeds the cohesive energy of bulk Pt ($-564\ kJ\,mol^{-1}$).[19] This has one important consequence: the anchored Pt^{2+} is thermodynamically stable against sintering, that is, the formation of metallic Pt nanoparticles. Therefore, we expect the anchored Pt^{2+} to be able to withstand high annealing temperatures. Actually, it would even be conceivable that the O^{2-} nanopockets may be able to abstract Pt atoms from supported Pt particles. We demonstrate the exothermicity of this pathway by DFT calculations (Figure 1 and S2). For Pt_9 particles on $Ce_{40}O_{80}$, for instance, abstraction of two Pt atoms is energetically favorable: the reaction yields two Pt^{2+} ions at the {100} nanofacets and four new Ce^{3+} centers, and leaves behind a Pt_7 aggregate. Whether such redispersion processes could be really observed in practice would, however, depend on the activation energies and the experimental conditions applied.

Two other aspects are exceptionally important to understand possible formation processes of the anchored Pt^{2+}. First, we have to ask whether the dispersed metal will act as a nucleation site for Pt nanoparticles. If this was the case, the Pt^{2+} would easily be covered by coexisting metallic Pt. To answer this question we investigate the formation of Pt_2 dimers, which is strongly exothermic ($369\ kJ\,mol^{-1}$)[20] on regular $CeO_2(111)$. In sharp contrast, the anchored Pt^{2+} does not favor bond formation with another Pt atom. No local minimum corresponding to a $Pt–Pt^{2+}/O_4$ moiety was found and during the geometry optimization the dimer dissociated into the Pt^{2+}/O_4 complex and a neutral Pt atom adsorbed nearby. This finding implies that the anchored Pt^{2+} species can actually coexist with metallic Pt nanoparticles without being buried by excess Pt. Notably, CO interacts very weakly with the anchored Pt^{2+} ion ($7\ kJ\,mol^{-1}$), indicating that the Pt^{2+} is hardly perturbed by CO adsorption.

A second important aspect is how the oxidation or reduction of ceria would influence the stability of the anchored Pt^{2+} ion. We investigate the adsorption of Pt at the {100} nanofacet of $Ce_{40}O_{80}$ under stepwise reduction of the NP by adsorption of H atoms (Figure 1 and S3). Upon hydrogenation of up to eight O atoms in the vicinity of the Pt^{2+}/O_4 complex ($Pt/Ce_{40}O_{72}(OH)_8$), the adsorption energy of the anchored Pt^{2+} decreases only slightly (to about $-600\ kJ\,mol^{-1}$, see Figure S3). However, further hydrogenation (12 hydrogenated O atoms in the vicinity of Pt^{2+}/O_4 moiety, $Pt/Ce_{40}O_{68}(OH)_{12}$) lowers the adsorption energy of the Pt atom below the metallic cohesion energy; in other words, the anchored Pt^{2+} ion becomes thermodynamically unstable with respect to formation of Pt nanoparticles. As could be expected, such strong reduction of ceria NP also induces the reduction of Pt^{2+} to Pt^0 (Figure 1, S1c, and S3). As a result, two Pt–O bonds are broken, the square-planar structure is lost, and the adsorption energy drops to $-328\ kJ\,mol^{-1}$, a much too weak binding to hinder Pt agglomeration. Indeed oxidized Pt finely dispersed on ceria was found to agglomerate upon heating to 600 °C in flowing H_2.[18] Our models now provide a microscopic picture of this phenomenon and elucidate its energetics.

The outlined theoretical modeling predicts that it should be possible to prepare very stable, atomically dispersed Pt^{2+} species at the surface of nanostructured CeO_2. Moreover, results of our current calculations indicate that the O_4 nanopockets also stabilize many other metals against agglomeration, such as Pd, Ni, Co, and Cu. Thus, this type of metal–support interaction appears to promote formation of single-metal-atom catalysts in a general fashion.

The cationic species which are formed, reside at the surface up to high temperature, withstanding sintering and diffusion into the bulk. This prediction can be tested by model catalytic experiments. In model catalysis we prepare well-defined surfaces under "ideal" conditions, that is, starting from atomically clean single-crystal surfaces under UHV conditions.[21] This strategy allows the building up of complex surfaces step by step, while at any stage these models remain accessible to the spectroscopic and microscopic methods of surface science.

We construct our model system starting from a well-ordered and fully stoichiometric $CeO_2(111)$ film prepared on Cu(111) (see Supporting Information for experimental details). Vapor deposition of active metals onto this surface is a standard method to prepare supported model catalysts.[12] However, the deposition of Pt, like other noble metals, on this surface typically leads to nucleation and growth of extended

NPs.[12] In view of our DFT data, this is not surprising since the ideal and ordered $CeO_2(111)$ surface does not provide the {100} nanofacets required to trap the metal in the form of cations. Therefore, we explore a new preparation method: the simultaneous co-deposition of Ce and Pt in an oxygen atmosphere (see Supporting Information for experimental details). Under the applied conditions, Ce is known to form CeO_2 NPs. We expect that the Pt should be incorporated into these particles during their growth and trapped as Pt^{2+} on their {100} nanofacets. Scanning tunneling microscopy (STM) studies of these surfaces show the growth of three-dimensional islands with an average diameter of approximately 3 nm and a typical height of around 0.4 nm (Figure 2a). Indeed, some aggregates reveal indications of a faceted shape which, not surprisingly, suggests epitaxial growth of the CeO_2 NPs on the $CeO_2(111)$ support. Figure 2b shows a schematic representation of these NPs. In spite of being terminated mainly by {111} facets, small {100} nanofacets can also be exposed, which may then accommodate the atomically dispersed Pt^{2+}.

To explore whether this is really the case, we perform synchrotron radiation photoelectron spectroscopy (SRPES) experiments (Figure 2c). Indeed, we detect no metallic Pt after deposition at low temperature (110 K), but ionic Pt exclusively in the oxidation states +2 and +4. Upon heating, the signal for Pt^{4+} rapidly decreases, indicating that the Pt^{4+} ion is rather unstable (in agreement with DFT calculations, Figure S1d). The Pt^{2+} species, however, behave as predicted by theory. They reveal exceptional thermal stability up to the highest temperatures that can be tested on our model surface (ca. 750 K). Note that the signal for Pt^{2+} even increases upon heating. In view of the fact that the spectra were taken with maximum surface sensitivity (photoelectron mean free path ca. 0.5 nm), this increase shows that the Pt^{2+} species are not lost by bulk diffusion but rather migrate to the very surface of the CeO_2 NPs. The critical role of providing the appropriate surface sites to anchor the Pt is demonstrated by the result of the second experiment shown in Figure 2d. In this case, we co-deposit several monolayer equivalents of CeO_2 and Pt under otherwise identical conditions. Upon heating, Pt^{2+} undergoes partial reduction and sinters to metallic NPs. Apparently, the multilayer film cannot provide a sufficiently large number of surface {100} nanopockets to anchor all deposited Pt. Those atoms which are located in the bulk or at unfavorable facets are bound too weakly to resist sintering to metallic nanoparticles.

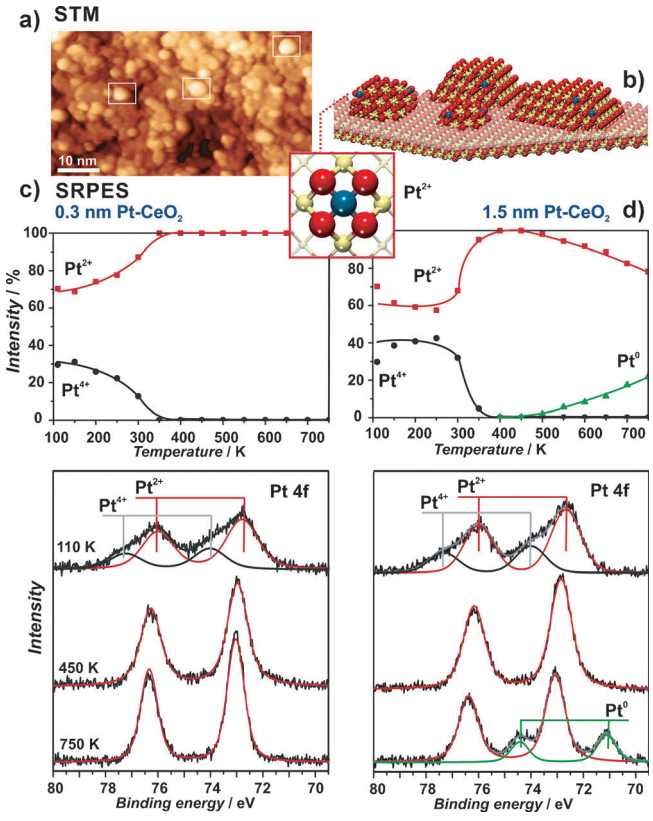

Figure 2. a) STM image obtained from Pt-CeO_2 nanoparticles grown on a well-ordered $CeO_2(111)$ surface under ultrahigh vacuum conditions followed by annealing to 700 K. White rectangles outline faceted Pt-CeO_2 particles. b) Schematic structure model of the model catalyst. c) Evolution of the Pt-4f core level spectra as a function of annealing temperature at a nominal Pt-CeO_2 film thickness of 0.3 nm (photon energy 180 eV); d) same as in (c) for a nominal Pt-CeO_2 film thickness of 1.5 nm. The intensities of Pt-4f spectra are normalized to unity.

While UHV model experiments impressively demonstrate the stability of the surface-anchored Pt^{2+} species, these experiments do not permit the preparation of materials at a scale large enough for real applications. However, this is possible by another thin-film deposition technique which is magnetron sputtering.[22] Although magnetron sputtering is a rather unconventional technique in catalyst preparation, it is scalable and routinely used in technological processes. Recently, we have shown that highly porous coatings can be prepared by magnetron sputtering implying a high application potential in catalysis.[23] Most interestingly, dispersed Pt-CeO_2 composites with any Pt:Ce ratio can be prepared by co-sputtering, in direct analogy to the model catalysts discussed above. We have also demonstrated the promising properties of the Pt-CeO_2 coating as electrocatalysts in proton exchange membrane fuel-cell technology, specifically their superior noble metal efficiency.[22,23] Recently we compared Pt-CeO_2 anodes with different Pt loadings between 0 and 10 μg Pt/cm^2 (see Supporting Information) The highest performance was shown for the catalyst with 2 μg Pt/cm^2 which contained Pt^{2+} ions only. For higher loading, Pt was in both the Pt^{2+} and the Pt^0 state and the performance of the catalyst was lower (Supporting Information, Figure S5). Even though the detailed reaction mechanisms could not yet be identified, our study clearly demonstrates that the Pt-CeO_2 electrocatalysts are extraordinarily active when only ionic platinum is present.

Herein, we prepare Pt-CeO_2 nanomaterials by co-sputtering onto graphite foil and characterize these materials by SRPES and high-resolution transmission electron microscopy (HRTEM, Figure 3). Indeed, SRPES reveals Pt in the oxidation states +2 and +4, as for the model catalysts. Note that spectra were again taken at low photon energy (180 eV), that is, with high surface sensitivity. Comparison with bulk-sensitive hard X-ray photoelectron spectra (HAXPES) indeed suggests that the Pt^{2+} species are preferentially located at the surface.[24]

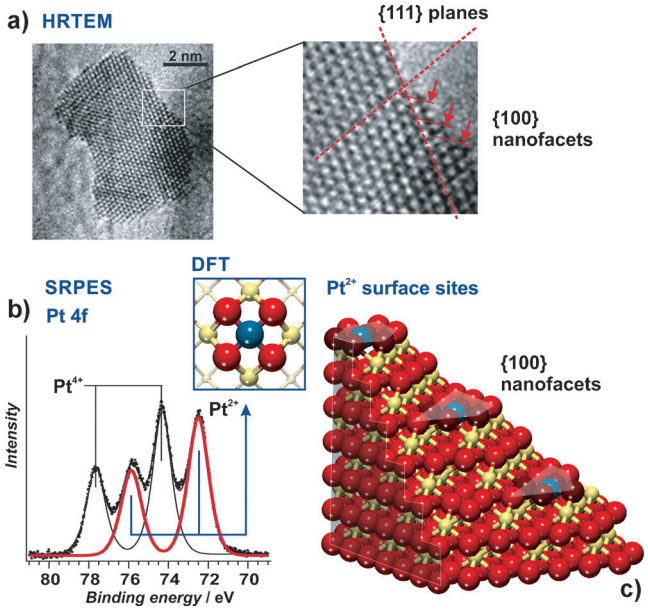

Figure 3. a) HRTEM image of Pt-CeO_2 particle chipped from a surface of 4% Pt-CeO_2 film prepared by magnetron sputtering. The arrows indicate {100} nanofacets; b) Pt-4f core level spectrum obtained from a Pt-CeO_2 nanoparticle film prepared by magnetron sputtering (photon energy 180 eV); c) model of a section of the Pt-CeO_2 particle illustrating the {100} nanofacets and the anchoring sites for Pt^{2+}.

Can we locate the {100} nanofacets on these materials where the Pt^{2+} species are anchored? A HRTEM image of a nanoparticle chipped from the surface of the 4% Pt-CeO_2 catalyst is shown in Figure 3a. The image corresponds to a Pt-CeO_2 particle, characterized by intersecting {111} and {100} CeO_2 crystal planes.

Apparently, the particle is decorated by a large number of small {100} terraces. Figure 3c shows a structure model of these facets and their alignment. These {100} nanofacets feature the square O_4 nanopockets that are required to anchor the Pt^{2+} centers. It is likely that the high adsorption energy of the anchored Pt^{2+} acts as an additional driving force to stabilize the {100} nanofacets during growth, thus contributing to the high density of these favorable structure elements on the Pt-CeO_2 NPs.

In conclusion, we have addressed the question how to use Pt, the most versatile and the most valuable noble metal in catalysis, with maximum possible efficiency. The strategy is simple: In our ideal material the noble metal must be atomically dispersed and located within the outermost surface layer only. In a catalytic reaction on such a material, every single Pt atom would then be accessible to the reactants. The challenge is to design a support material that stabilizes the atomically dispersed surface Pt species under reaction conditions. By means of DFT modeling we identify a structural element on nanostructured ceria which holds the potential to build such a material. It is a Pt^{2+} ion located inside a square pocket of O^{2-} ions at a {100} nanofacet of CeO_2. For this structural unit, theory predicts the adsorption energy of the dispersed Pt to be large enough to withstand thermally induced aggregation to metallic nanoparticles and loss of Pt by diffusion into the ceria bulk. Once prepared, the surface-anchored Pt^{2+} should be stable, even under harsh conditions. In well-controlled surface-science experiments, we have prepared model systems for the nanostructured ceria with surface-anchored Pt^{2+}. On this model we show that the Pt^{2+} is indeed located at the very surface and remains perfectly stable up to high temperature without reduction, sintering, or bulk diffusion. To bring this result closer to applications, we have prepared CeO_2 nanomaterials with atomically dispersed Pt by magnetron sputtering. The Pt-CeO_2 nanomaterials reveal ionic Pt^{2+} surface species, very similar to those in the model experiments. By high resolution electron microscopy, we have identified the highly abundant CeO_2{100} nanofacets on these materials which host the anchored Pt^{2+} species. Our on-going fuel-cell tests using anode catalysts based on these Pt-CeO_2 nanomaterials show very high performance when Pt is present exclusively in the 2+ state.

Our study shows how atomic-level insights help to design noble-metal-efficient materials on a knowledge-driven basis. Materials such as the atomically dispersed Pt-CeO_2, may play a key role in reducing the demand for critical materials in future applications.

Received: February 12, 2014
Published online: June 11, 2014

Keywords: ceria nanoparticles · density functional calculations · heterogeneous catalysis · model catalyst · platinum

[1] a) G. Ertl, H. Knözinger, F. Schüth, J. Weitkamp, *Handbook of Heterogeneous Catalysis*, 2nd ed., Wiley-VCH, Weinheim, **2008**; b) K. Yamamoto, T. Imaoka, W.-J. Chun, O. Enoki, H. Katoh, M. Takenaga, A. Sonoi, *Nat. Chem.* **2009**, *1*, 397–402; c) G. A. Somorjai, D. W. Blakely, *Nature* **1975**, *258*, 580–583; d) R. D. Gillard, *Nature* **1968**, *218*, 502–503; e) V. W. W. Yam, *Nat. Chem.* **2010**, *2*, 790–790.
[2] J. M. Thomas, *J. Chem. Phys.* **2008**, *128*, 182502.
[3] J. Tollefson, *Nature* **2007**, *450*, 334–335.
[4] a) W. Vielstich, A. Lamm, H. A. Gasteiger, *Handbook of Fuel Cells: Fundamentals, Technology, Applications*, Wiley, Chichester, **2003**; b) V. R. Stamenkovic, B. S. Mun, M. Arenz, K. J. J. Mayrhofer, C. A. Lucas, G. F. Wang, P. N. Ross, N. M. Markovic, *Nat. Mater.* **2007**, *6*, 241–247.
[5] H. S. Gandhi, G. W. Graham, R. W. McCabe, *J. Catal.* **2003**, *216*, 433–442.
[6] a) H. T. Chung, J. H. Won, P. Zelenay, *Nat. Commun.* **2013**, *4*, 1922; b) W. Yang, T.-P. Fellinger, M. Antonietti, *J. Am. Chem. Soc.* **2011**, *133*, 206–209; c) A. Le Goff, V. Artero, B. Jousselme, P. D. Tran, N. Guillet, R. Métayé, A. Fihri, S. Palacin, M. Fontecave, *Science* **2009**, *326*, 1384–1387.
[7] G. Armstrong, *Nat. Chem.* **2013**, *5*, 809–809.
[8] M. Cargnello, V. V. T. Doan-Nguyen, T. R. Gordon, R. E. Diaz, E. A. Stach, R. J. Gorte, P. Fornasiero, C. B. Murray, *Science* **2013**, *341*, 771–773.
[9] a) J. H. Kwak, J. Z. Hu, D. Mei, C. W. Yi, D. H. Kim, C. H. F. Peden, L. F. Allard, J. Szanyi, *Science* **2009**, *325*, 1670–1673; b) Y. P. Zhai, D. Pierre, R. Si, W. L. Deng, P. Ferrin, A. U. Nilekar, G. W. Peng, J. A. Herron, D. C. Bell, H. Saltsburg, M. Mavrikakis, M. Flytzani-Stephanopoulos, *Science* **2010**, *329*, 1633–1636; c) B. T. Qiao, A. Q. Wang, X. F. Yang, L. F. Allard, Z. Jiang, Y. T. Cui, J. Y. Liu, J. Li, T. Zhang, *Nat. Chem.* **2011**, *3*, 634–641.

[10] Q. Fu, H. Saltsburg, M. Flytzani-Stephanopoulos, *Science* **2003**, *301*, 935 – 938.
[11] a) M. Flytzani-Stephanopoulos, B. C. Gates, *Annu. Rev. Chem. Biomol. Eng.* **2012**, *3*, 545 – 574; b) X. F. Yang, A. Q. Wang, B. T. Qiao, J. Li, J. Y. Liu, T. Zhang, *Acc. Chem. Res.* **2013**, *46*, 1740 – 1748; c) M. Flytzani-Stephanopoulos, *Acc. Chem. Res.* **2014**, 47, 783 – 392.
[12] G. N. Vayssilov, Y. Lykhach, A. Migani, T. Staudt, G. P. Petrova, N. Tsud, T. Skala, A. Bruix, F. Illas, K. C. Prince, V. Matolin, K. M. Neyman, J. Libuda, *Nat. Mater.* **2011**, *10*, 310 – 315.
[13] a) A. Migani, G. N. Vayssilov, S. T. Bromley, F. Illas, K. M. Neyman, *J. Mater. Chem.* **2010**, *20*, 10535 – 10546; b) A. Migani, K. M. Neyman, S. T. Bromley, *Chem. Commun.* **2012**, *48*, 4199 – 4201; c) F. Zhang, Q. Jin, S.-W. Chan, *J. Appl. Phys.* **2004**, *95*, 4319 – 4326.
[14] M. M. Branda, R. M. Ferullo, M. Causa, F. Illas, *J. Phys. Chem. C* **2011**, *115*, 3716 – 3721.
[15] A. Bruix, K. M. Neyman, F. Illas, *J. Phys. Chem. C* **2010**, *114*, 14202 – 14207.
[16] A. G. Hu, K. M. Neyman, M. Staufer, T. Belling, B. C. Gates, N. Rösch, *J. Am. Chem. Soc.* **1999**, *121*, 4522 – 4523.
[17] F. A. Cotton, G. Wilkinson, *Advanced Inorganic Chemistry*, 5th ed., Wiley, New York, **1990**.
[18] Y. Nagai, T. Hirabayashi, K. Dohmae, N. Takagi, T. Minami, H. Shinjoh, S. Matsumoto, *J. Catal.* **2006**, *242*, 103 – 109.
[19] C. Kittel, *Introduction to Solid State Physics*, 5th ed., Wiley, New York, **1976**.
[20] A. Bruix, F. Nazari, K. M. Neyman, F. Illas, *J. Chem. Phys.* **2011**, *135*, 244708.
[21] a) G. Ertl, *Angew. Chem.* **2008**, *120*, 3578 – 3590; *Angew. Chem. Int. Ed.* **2008**, *47*, 3524 – 3535; b) S. Schauermann, N. Nilius, S. Shaikhutdinov, H.-J. Freund, *Acc. Chem. Res.* **2013**, *46*, 1673 – 1681; c) H. Kuhlenbeck, S. Shaikhutdinov, H.-J. Freund, *Chem. Rev.* **2013**, *113*, 3986 – 4034.
[22] V. Matolín, I. Matolínová, M. Václavů, I. Khalakhan, M. Vorokhta, R. Fiala, I. Piš, Z. Sofer, J. Poltierová-Vejpravová, T. Mori, V. Potin, H. Yoshikawa, S. Ueda, K. Kobayashi, *Langmuir* **2010**, *26*, 12824 – 12831.
[23] V. Matolín, R. Fiala, I. Khalakhan, J. Lavková, M. Václavů, M. Vorokhta, *Int. J. Nanotechnol.* **2012**, *9*, 680 – 694.
[24] I. Matolínová, R. Fiala, I. Khalakhan, M. Vorokhta, Z. Sofer, H. Yoshikawa, K. Kobayashi, V. Matolín, *Appl. Surf. Sci.* **2012**, *258*, 2161 – 2164.

